

Measuring variation in EMD reduction with location in primary alkaline batteries

A. URFER, G. A. LAWRENCE*, D. A. J. SWINKELS

Department of Chemistry, The University of Newcastle, Callaghan NSW 2308, Australia

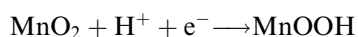
Received 24 June 1996; revised 18 December 1996

Reduction of manganese dioxide is not uniform throughout alkaline cells with thick cathodes. Quantification of the degree of reduction of MnO_2 as a function of location in the cathode by determining the degree of EMD reduction in discharged alkaline cathodes is described, using a new experimental technique which allows collection and analysis of regionally defined electrolytic manganese dioxide (EMD) samples from commercial primary alkaline batteries of different sizes. This method has been developed for 1.5 V D-size and C-size alkaline batteries. The information gained can be used to better explain the behaviour of real cells with thick cathodes.

1. Introduction

Primary alkaline batteries containing manganese dioxide as the active cathode material were investigated. Electrolytic manganese dioxide (EMD) is well known as an excellent electrode material and has been found to be the form of manganese dioxide that is most suitable as the positive active material in alkaline cells [1]. EMD is inexpensive and has the ability to maintain high discharge rates, a good performance over a wide temperature range and has a long storage life. Therefore, EMD is the most widely used cathode material for alkaline primary batteries and has also found application in rechargeable batteries [2].

EMD is not a single compound, but a rather large family of closely related compounds whose physical and chemical properties can be made to vary significantly by changing the conditions of electrodeposition [3, 4]. There exists a range of structural forms with mostly nonstoichiometric compositions MnO_x with $x < 2$, and a typical EMD would have a chemical composition similar to $\text{MnO}_{1.96}\text{H}_{0.08}$ on a dry basis. It is generally accepted that in alkaline electrolyte manganese dioxide discharges by abstraction of a proton from the concentrated potassium hydroxide electrolyte and reception of an electron from an external circuit:



The proton–electron pair formed during the discharge diffuses away from the EMD surface to the interior of the material [5]. The rate at which this proton–electron pair diffuses is limited by the ability of the proton to move through the solid and is a function of the structural, chemical, physical and electrochemical properties of the EMD.

Based on mathematical model predictions and general observations relating to alkaline cells with thick cathodes, it is generally accepted that the reduction of MnO_2 is not uniform throughout the cathode. Preisler carried out a brief study on this subject, but his experimental attempt to quantify these effects in real cells remains the only study reported to date [6]. The scope of his work was limited and some questions remain concerning the experimental technique, for example, whether the cathode samples were removed from the cell quickly enough after discharge to avoid any re-equilibration.

In this paper, a rapid and relatively easy method of collecting well defined samples from a discharged battery is described. Using commercial primary alkaline Duracell® batteries of different sizes, the degree of EMD reduction in alkaline cathodes as a function of location in the cathode and discharge rate can be defined. The cells have been discharged either at constant current or constant resistance at different rates before being frozen in liquid nitrogen immediately after discharge. Samples were extracted from the cathode at various locations and were analysed to determine x in MnO_x . Although it is not in the scope of this paper to simulate discharges of real cells, the information gained through this work can be used to check some of the predictions of Cheh's model [7–12] as well as to better explain the behaviour of real cells with thick cathodes. This is currently under investigation [13].

2. Experimental details

Well characterized test cells were discharged under controlled conditions of continuous drain (constant current or constant resistance) at $21^\circ\text{C} \pm 2^\circ\text{C}$. As soon as the desired end voltage of 900 mV or 800 mV, respectively, was reached, the cells were immediately frozen in liquid nitrogen to prevent equilibration within the cathodes. After collection of EMD

* Author to whom correspondence should be addressed.

samples from various cathode locations, these samples were analysed to determine the reduction degree of the manganese dioxide as x in MnO_x . The technique has been developed for both the larger D-size and smaller C-size cells.

2.1. Discharge setup (hardware and software)

The discharge setup comprised an IBM-compatible computer equipped with a high performance data acquisition card PC-LabCard PCL-818 (maximum input range of ± 10 V) which read up to eight differential analog input channels. Connection blocks for the PCL-818 were provided by the universal screw terminal daughter board PCLD-780 which was mounted in a protective instrument case. The control software was written in Microsoft QuickBasic 4.0 using the PCL driver version 1.0.

One or two batteries were discharged using this basic setup for both constant current and constant resistance discharges using an EG&G Princeton Applied Research model 362 scanning potentiostat or the required resistor, respectively. Readings of the PCL-818 data acquisition card were values between 0 and 4096 which had to be converted into potentials. These potentials were averaged over a user-defined period of time (typically 30 s) and the averaged potentials were periodically saved in data files as data pairs of the form: time (s), potential (mV). The data were processed using Microsoft Excel 4.0.

2.2. Discharge of alkaline batteries

Three different sets of especially selected D-Size and C-size batteries have been investigated. These batteries were manufactured and supplied by Duracell® and details are given in Table 1. All discharges were continuous drain.

2.2.1. D-size batteries containing electrolytic manganese dioxide (type A) were subjected to a high drain discharge at a constant current of 1.0 A.

2.2.2. D-size batteries were discharged at constant resistance of 4.7Ω (medium drain).

2.2.3. C-size batteries containing electrolytic manganese dioxide (type B) were discharged at constant resistance of 10Ω (medium drain).

2.3. EMD sample collection

Each battery was discharged at constant drain until its desired end voltage was reached. The progress was monitored by computer and as soon as the discharge was finished, the PVC sleeve label as well as the positive cap were immediately removed. After the battery can had been labelled, the battery was immersed in liquid nitrogen and chilled completely. Subsequently, all operations were done in the frozen state and the battery could only be handled with special insulated gloves.

About 5 mm of the battery's negative end was cut off with a bandsaw in order to remove its negative cap including the plastic grommet. The closer this cut was to the battery's plastic grommet, the more cathode material was available for collection. It proved to be best not to cut the positive end of the can, since this reduced deformation of the steel can on mounting in the lathe.

After this procedure, the battery was refrozen. Then it was mounted in a lathe with the open end facing outwards. After removal of the nail which collects the anode current, the anode was drilled out with a chilled 20.64 mm (13/16 inch) borer in the case of a D-size battery and with a chilled 14.29 mm (9/16 inch) borer in the case of a C-size battery respectively. A professional tooling system called 'T-MAXU' from Sandvik Coromant consisting of a solid steel boring bar (S10K-STFCR 09) which holds clamped triangular tips (TCMT 09 02 04-UR H13A) with a strong cutting edge was used to cut the frozen EMD cathode. The battery was fixed in the lathe, the cutting tool was lined up and collection of the samples commenced with a lathe rotating speed of 495 rpm from the inside of the cathode. After each EMD sample ring had been pared off, the battery was removed and the loose EMD was collected and stored in a labelled sample container. Before the battery was mounted again to take the next sample, it was refrozen in liquid nitrogen. The actual samples themselves were not kept frozen, but were immediately analysed to minimize reoxidation. It was found that, depending on the cutting edge of the tip, eight to ten concentric rings of samples could be collected.

2.4. Analysis of collected EMD samples

To quantify the progress of the reduction of the EMD throughout the cathode ring, the value for x in

Table 1. Cathode dimensions and weights

Test series	size	cathode weight /g	EMD /%	MnO_2 /%	MnO_2 /g	Capacity* /Ah	Cathode thick† /mm
2.2.1	D	66.7	85	89.6	50.8	15.6(5)	5.12
2.2.2	D	66.6	84	89.6	50.2	15.4(5)	5.12
2.2.3	C	32.5	84	89.2	24.3	7.5(0)	3.90

* Calculated for a one electron change.

† New, undischarged battery.

MnO_x was determined using an automated analytical method [14–17] based on dissolving the sample in 0.05 M (NH₄)₂SO₄·FeSO₄·6H₂O solution with 4% (v/v) sulfuric acid and titrating with KMnO₄ to determine total oxidizing power and total Mn in the sample.

3. Results and discussion

3.1. EMD sample collection

Basically, there are two approaches to collect concentric ring samples from the cathode, either from the outside towards the centre of the battery or from the centre towards the outer layers of the battery. Both methods were tried, but with ongoing use of these techniques it became clear that the latter procedure allowed a cleaner separation of the more important inner layers. Because the frozen cathode gets thinner during sample collection as each ring of sample is removed, its structural stability decreased, to the point where the remaining EMD finally collapsed, which yielded a final sample containing bigger and less uniform fragments. Since the region of EMD closest to the anode discharged more rapidly (and was therefore of greater interest) than EMD located at the outside of the cell, a cleaner collection of inner samples was desired and only given by the second practice. Additionally, EMD collection was more quantitative. Hence, only results employing this second method are described here.

It proved to be difficult to find a wear resistant tip which kept its sharpness during EMD samples collection from any frozen cathode. A strong tip material was important for two reasons. First, to have a better control of the exact EMD layer thickness, and second, to prevent the cathode from breaking. The latter led to coarse cathode fragments which made the determination of *x* in MnO_x less precise because they were not as representative of the whole sample as was the case for samples consisting of fine particles. Therefore, a tip was needed which wore only slowly during the cutting process. Initially, a homemade toolbar with soldered tips was used and different tip materials were investigated including tool steel, tungsten carbide and a combination of titanium nitride, aluminium oxide and titanium carbide. All the different tips had to be regularly sharpened to maintain a sharp cutting edge. This tool was subsequently replaced by a professional Sandvik Coromant tooling system consisting of a solid steel boring bar which held triangular tungsten carbide tips. For every battery, a new tip edge was used to minimize effects of wear and tear. A diameter of 13 mm was a minimum requirement for drilled holes in batteries. Another measure to help protect the tip was the reduction of the rotation speed of the lathe from 1840 to 770 rpm and ultimately to 495 rpm.

For all samples, a constant layer thickness of about 0.4 mm (C-size batteries) or 0.6 mm (D-size

batteries) was removed, yielding eight to ten samples per battery. In all cases, the final sample was much bigger than all previous samples, for reasons described above. For D-size batteries, the layer thicknesses of the collected samples could only be based on the lathe readings, but for C-size batteries, a more accurate method which used the weights of samples was developed to better determine actual layer thicknesses. Since the samples were collected radially from the inside towards the outside, they increased in mass in direct proportion to the area, which itself depended on the layer thickness. The thickness Δr_n of any sample is given by

$$m_n = C \times (r_n^2 - r_{n-1}^2) \rightarrow r_n = \sqrt{\frac{m_n}{C} + r_{n-1}^2} \\ \rightarrow \Delta r_n = r_n - r_{n-1} \quad (1)$$

where m_n is the mass of the *n*th sample, $C = m_{\text{tot}}(r_o^2 - r_i^2)^{-1}$, m_{tot} is the entire mass of all collected cathode samples, r_o and r_i are the outer and inner radii of the cathode, respectively.

In the case of the C-size battery, the cathode inner diameter was 16.89 mm ($r_i = 8.445$ mm) and the cathode outer diameter was 24.69 mm ($r_o = 12.345$ mm) which gave a pellet thickness of 3.90 mm. These values were related to a new, undischarged battery and were only an approximation for the case of a discharged battery. Since the pellet expanded during the discharge by an unknown amount, the inner diameter became smaller whereas the outer diameter was invariable. Since the exact value r_i for the discharged cell was unknown, the original value of 8.445 mm was used in our calculations. The value *C* includes the cathode pellet's density, its height and π . Obviously, its value was only correct when the cathode material was quantitatively or nearly quantitatively collected, which was the case with our sample acquisition technique. The total mass m_{tot} differed from battery to battery because of variable cathode heights due to the initial cut.

3.2. Analysis of collected EMD samples

Determination of the degree of reduction in EMD employed two redox titrations. The method was based on detecting the iron(II)/iron(III) redox potential and the manganese(II)/manganese(III) redox potential, the latter stabilized as a pyrophosphate species, respectively. The first titration was relatively quick since the potential equilibration was obtained within seconds of addition of KMnO₄. In contrast, the second titration took much longer to reach its equilibrium state (minutes). The titration was speeded up by two measures. First, permanganate was added in small steps at fairly short intervals without awaiting a fully steady potential reading. As long as the titration had not reached the equivalence point, the potential increased after addition of oxidant before it decreased again. As soon as the equivalence point was attained the potential increased steadily and did not decrease any more. When the computer

detected this potential behaviour, the titration was deemed finished.

Second, to further improve the efficiency of the titrations, the samples were titrated in batches. Instead of determining the x values for every sample in turn, all the samples were prepared together and the first titration was completed for all of them. After the first titration of the first sample was finished, the tetrasodium pyrophosphate was added. While the salt was dissolving, the first titration with the second sample was carried out and so on. By the time the first titration was finished with the last of the samples, the first sample was ready for the second titration. It was found that duplicates of titrations lay within ± 0.01 ml.

It was important to analyse alkaline samples for their x in MnO_x content within hours of their collection. During the course of this work, it was found that properly prepared EMD samples, stored in sealed containers at room temperature, slowly re-oxidized on standing. This trend could neither be stopped by storing the samples under vacuum nor in a freezer at -20°C . In all investigated cases, EMD reduction degree determinations which were not carried out on the same day the discharge was terminated showed an increased, and hence wrong, x value. Consequently, samples of discharged batteries could not be kept for any long periods of time.

A more detailed follow up of samples from a discharged battery is summarized in Fig. 1. The samples were stored in a freezer at -20°C for the first seven days and they were kept in air afterwards. After 0, 1, 2, 3, 6, 7, 8, 10, 14, 21 and 28 days the containers were briefly opened to remove small samples for the immediate determination of x in MnO_x . It seems that freezing slowed down the reoxidation but it could not prevent it from happening. Also, the rate of reoxidation appears to be different for different samples of the same battery. The explanation for this behaviour is unclear, but may relate to different sizes of cathode mix shavings presenting different surface areas for air oxidation.

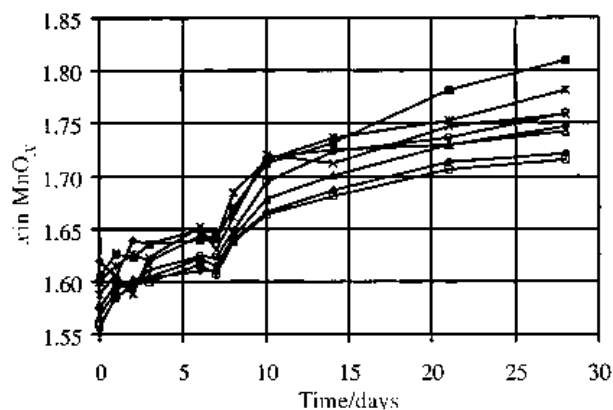


Fig. 1. Reoxidation of reduced samples (1 to 8) in a freezer (-20°C) for seven days, then in air (20°C) thereafter. Samples: (□)1, (◆)2, (Δ)3, (○)4, (×)5, (*)6, (■)7 and (◆)8.

Analyses of samples from undischarged batteries gave reference values for x in MnO_x in the range of 1.94 to 1.95. These numbers were typical for new batteries. Notably, no unexpected behaviour was found for the undischarged samples, where the same x values have been determined even after weeks of storage in air at room temperature.

3.3. Discharge of alkaline batteries

3.3.1. D-size batteries were discharged at a constant current of 1.0 A, which is a very high drain rate. The continuous discharge of eight batteries to 900 mV gave a discharge time of (5.2 ± 0.4) h and the continuous discharge of three batteries to 800 mV took (6.1 ± 0.3) h. In terms of capacities, the values for the discharges were (5.2 ± 0.4) Ah and (6.1 ± 0.3) Ah, respectively, and expressed as faraday per mole of $\text{MnO}_{2.00}$ the values were (0.33 ± 0.02) faraday mol^{-1} and (0.39 ± 0.02) faraday mol^{-1} , respectively. Batteries tested with a higher drain rate of 1.07 A gave average values of (3.4 ± 0.8) h, (3.7 ± 0.9) Ah and (0.24 ± 0.06) faraday mol^{-1} . With high drains it was found that the inner cylinder of the cathode was much more discharged than the outer cylinder as illustrated in Fig. 2. This indicates that the batteries were not efficiently discharged.

3.3.2. D-size batteries were also discharged through $4.7\ \Omega$ resistors to 800 mV. For six batteries a discharge time of (48.9 ± 1.2) h was observed. The discharge curve, averaged for six batteries, is illustrated in Fig. 3.

To determine the capacities Q of batteries, the area under the curve was calculated using the trapezoidal method. The capacity was found to be (11.9 ± 0.3) Ah or (0.75 ± 0.02) faraday mol^{-1} .

Analyses of the reduction degree for individual samples of three of these batteries gave the results illustrated in Fig. 2. It can be clearly seen that medium drain discharges were much more efficient than high drain discharges described earlier.

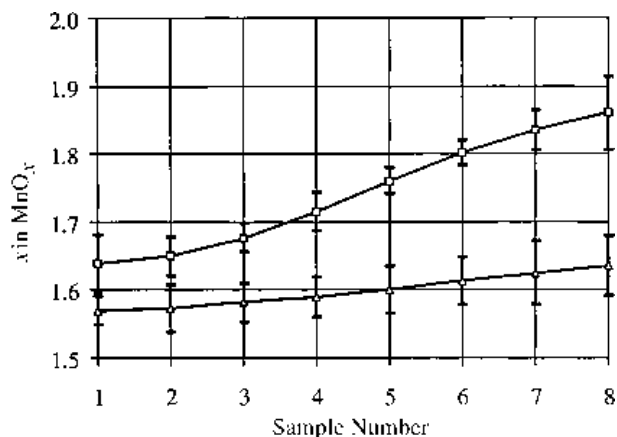


Fig. 2. Average x in MnO_x and 2 SD bars for D-size batteries following high drain discharge at 1.0 A to 800 mV (□) and medium drain discharge through $4.7\ \Omega$ to 800 mV (Δ).

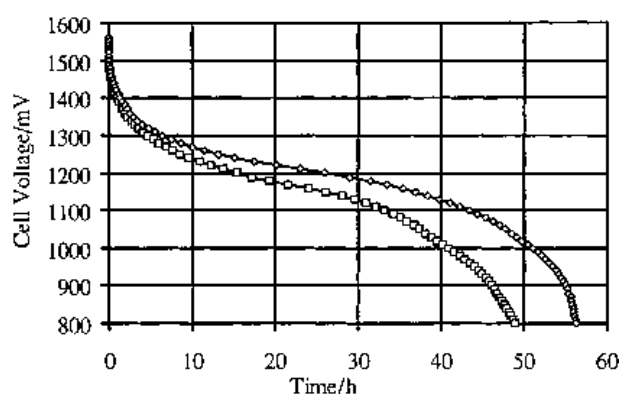


Fig. 3. Averaged discharge curves for D-size (\square , $R = 4.7 \Omega$) and C-size (\diamond , $R = 10 \Omega$) batteries.

3.3.3. For the discharge of four C-size batteries through 10Ω resistors to 800 mV a discharge time of $(56.3 \pm 1.5) \text{ h}$ was observed. The discharge data for all batteries were averaged, and the resulting discharge curve is shown in Fig. 3. The total capacity Q , was found to be $(6.4 \pm 0.1) \text{ Ah}$ or $(0.85 \pm 0.02) \text{ faraday mol}^{-1}$.

The data for both C-size and D-size batteries are summarized in Table 2.

The x in MnO_x data for four C-size cells are given in Fig. 4.

For each experimental point an error of $\pm 0.1 \text{ mm}$ for the sample thickness and ± 0.01 for x values has to be taken into consideration. Note that EMD utilization is more uniform than for the D-size cells due to the thinner cathodes in C-cells and the slower rate of discharge used for these cell. The results suggest that there is increased EMD utilization at both the inner and the outer radii of the cathode. Based on cathode modelling work this type of behaviour is expected to occur when the ionic and electronic conductivities within the cathode are similar in magnitude [7–12]. While the electronic conductivity is initially an order of magnitude higher than the ionic conductivity it may well be that as discharge progresses and the cathode swells the electronic conductivity provided by the graphite is reduced to a level close to the ionic conductivity. This requires further investigation.

4. Conclusions

Two closely related methods have been investigated to collect concentric rings of EMD samples from commercial alkaline batteries. The method where

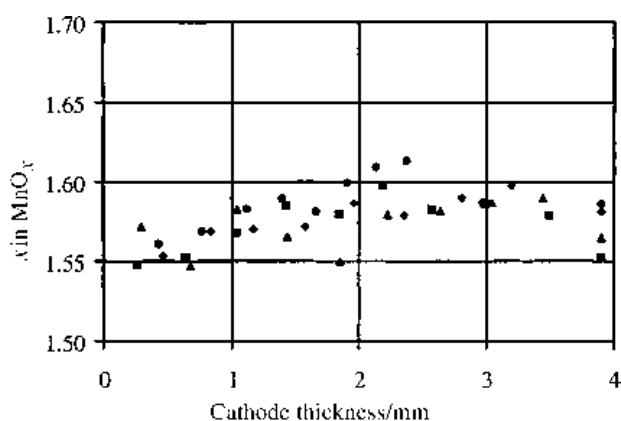


Fig. 4. x in MnO_x values for four C-size batteries following medium drain discharge through 10Ω to 800 mV .

EMD was collected from the inside to the outside in a series of concentric rings proved superior and reproducible. The method was shown to be suitable for both D-size and C-size batteries.

Using the paring method developed in this study, a limited number of Duracell® batteries were investigated. Batteries were discharged, sampled, and computer controlled potentiometric titrations were used to determine the reduction degree x in MnO_x as a function of radial position in the cathodes. It was found that collected samples from discharged batteries reoxidized over time when exposed to air and this process could not be stopped by storing the samples in a freezer or in a vacuum desiccator. Thus the only way to obtain accurate results was by analysis of all samples on the same day.

From our experiments, it can be seen that EMD discharged more uniformly (hence more efficiently) throughout the cathode in C-size cells compared with D-size cells, as was expected based on the thinner cathode in C-size cells and the slower rate of discharge.

In summary, an effective and relatively simple method for analysis of the spatial distribution of discharge in commercial alkaline batteries has been established which can be used to better explain the discharge behaviour of these cells.

Acknowledgements

The authors gratefully acknowledge sponsorship by the Australian Manganese Company Proprietary Limited (AMCL), Duracell® and the Australian Research Council (ARC).

Table 2. Discharge data for C-size and D-size batteries (to 800 mV)

Batteries	Time /h	Capacity /Ah	Change /faraday mol^{-1}	x in MnO_x (theoretical)	x in MnO_x (measured)
D-size*	48.9 ± 1.2	11.9 ± 0.3	0.75 ± 0.02	—	—
C-size†	56.3 ± 1.5	6.4 ± 0.1	0.85 ± 0.02	1.58 ± 0.01	1.58 ± 0.01

* Average of six batteries.

† Average of four batteries.

References

- [1] K. V. Kordesch, 'Batteries', vol.1, (edited by K. V. Kordesch), Marcel Dekker, New York (1974), chapter 2.
- [2] K. V. Kordesch and M. Weissenbacher, *J. Power Sources* **51** (1994) 61.
- [3] T. N. Anderson, *Prog. Batteries & Battery Mater.* **11** (1992) 105.
- [4] R. P. Williams, R. A. Fredlein, G. A. Lawrence, D. A. J. Swinkels and C. B. Ward, *ibid.* **12** (1993) 102.
- [5] F. L. Tye, 'Manganese Dioxide Electrode Theory and Practice for Electrochemical Applications', The Electrochemical Society, Pennington, NJ (1985), p. 301.
- [6] E. Preisler, *Prog. Batteries & Solar Cells* **9** (1990) 21.
- [7] C. Y. Mak, H. Y. Cheh, G. S. Kelsey and P. Chalilpoyil, *J. Electrochem. Soc.* **138** (1991) 1607.
- [8] *Idem, ibid.* **138** (1991) 1611.
- [9] J.-S. Chen and H. Y. Cheh, *ibid.* **140** (1993) 1205.
- [10] *Idem, ibid.* **140** (1993) 1213.
- [11] E. J. Podlaha and H. Y. Cheh, *ibid.* **141** (1994) 15.
- [12] *Idem, ibid.* **141** (1994) 28.
- [13] T. D. Farrell and D. A. J. Swinkels, unpublished results
- [14] J. Lingane, R. Karplus, *Ind. Eng. Chem., Anal. Ed.* **18** (1946) 191.
- [15] K. J. Vetter, N. Jaeger, *Electrochem. Acta* **11** (1966) 401.
- [16] W. C. Maskell, private communication to S. W. Donne (1992).
- [17] S. W. Donne, PhD thesis, University of Newcastle, Australia (1996).